Trajectories of imaging markers in brain aging

the Rotterdam Study

Vinke, Elisabeth J.; de Groot, Marius; Venkatraghavan, Vikram; Klein, Stefan; Niessen, Wiro J.; Ikram, M. Arfan; Vernooij, Meike W.

DOI
10.1016/j.neurobiolaging.2018.07.001

Publication date
2018

Document Version
Final published version

Published in
Neurobiology of Aging

Neurobiology of Aging 71 (2018) 32–40

Contents lists available at ScienceDirect

Neurobiology of Aging

journal homepage: www.elsevier.com/locate/neuaging

Trajectories of imaging markers in brain aging: the Rotterdam Study

Elisabeth J. Vinke [a], Marius de Groot [a,b,c], Vikram Venkatraghavan [a,c], Stefan Klein [a,c], Wiro J. Niessen [a,c,e], M. Arfan Ikram [a,b,d,1], Meike W. Vernooij [a,b,*,1]

[a] Department of Radiology and Nuclear Medicine, Erasmus MC University Medical Center, Rotterdam, The Netherlands
[b] Department of Epidemiology, Erasmus MC University Medical Center, Rotterdam, The Netherlands
[c] Department of Medical Informatics, Erasmus MC University Medical Center, Rotterdam, The Netherlands
[d] Department of Neurology, Erasmus MC University Medical Center, Rotterdam, The Netherlands
[e] Department of Imaging Physics, Faculty of Applied Sciences, Delft University of Technology, Delft, The Netherlands

ARTICLE INFO

Article history:
Received 16 January 2018
Received in revised form 9 June 2018
Accepted 1 July 2018
Available online 17 July 2018

Keywords:
MRI
Diffusion-MRI
White matter
Gray matter
Neurodegeneration
Epidemiology
Population-based
Longitudinal

ABSTRACT

With aging, the brain undergoes several structural changes. These changes reflect the normal aging process and are therefore not necessarily pathologic. In fact, better understanding of these normal changes is an important cornerstone to also disentangle pathologic changes. Several studies have investigated normal brain aging, both cross-sectional and longitudinal, and focused on a broad range of magnetic resonance imaging (MRI) markers. This study aims to comprise the different aspects in brain aging, by performing a comprehensive longitudinal assessment of brain aging, providing trajectories of volumetric (global and lobar; subcortical and cortical), microstructural, and focal (presence of microbleeds, lacunar or cortical infarcts) brain imaging markers in aging and the sequence in which these markers change in aging. Trajectories were calculated on 10,755 MRI scans that were acquired between 2005 and 2016 among 5286 persons aged 45 years and older from the population-based Rotterdam Study. The average number of MRI scans per participant was 2 scans (ranging from 1 to 4 scans), with a mean interval between MRI scans of 3.3 years (ranging from 0.2 to 9.5 years) and an average follow-up time of 5.2 years (ranging from 0.3 to 9.8 years). We found that trajectories of the different volumetric, microstructural, and focal markers show nonlinear curves, with accelerating change with advancing age. We found earlier acceleration of change in global and lobar volumetric and microstructural markers in men compared with women. For subcortical and cortical volumes, results show a mix of more linear and nonlinear trajectories, either increasing, decreasing, or stable over age for the subcortical and cortical volume and thickness. Differences between men and women are visible in several parcellations; however, the direction of these differences is mixed. The presence of focal markers show a nonlinear increase with age, with men having a higher probability for cortical or lacunar infarcts. The data presented in this study provide insight into the normal aging process in the brain, and its variability.

1. Introduction

The aging brain undergoes various structural changes, which can manifest themselves clinically in corresponding functional changes. Much research has been dedicated to understanding these brain changes because these do not only inform about healthy brain aging, but also provide a reference point against which pathologic changes can be contrasted.

The development of noninvasive imaging techniques has fueled research into the aging brain in healthy individuals. Since magnetic resonance imaging (MRI) was first introduced in biomedical research in the 1980s, several pioneers performed small studies using this novel technique to assess macrostructural brain changes in aging (Gur et al., 1991; Jernigan et al., 1990, 1991; Krishnan et al., 1990; Pfefferbaum et al., 1994; Sullivan et al., 1995). After approximately one decade, large cross-sectional studies and population-based studies followed to inform about, for example, sex differences and brain changes in a large sample of healthy volunteers, instead of specific control subjects (Coffey et al., 1998; Good et al., 2001; Mu et al., 1999). Simultaneous developments in MRI scanners and software increased the accuracy of structural (volumetric)

* Corresponding author at: Department of Epidemiology, Erasmus University Medical Center, PO Box 2040, Rotterdam, 3000 CA, The Netherlands. Tel.: +31 10 70 42006; fax: +31 10 70 446 57.
E-mail address: m.vernooij@erasmusmc.nl (M.W. Vernooij).
[1] Denotes equal contribution.

https://doi.org/10.1016/j.neurobiolaging.2018.07.001

measurements and enabled measuring microstructural (white matter organization) changes in aging (Coupe et al., 2017; Cox et al., 2016; de Groot et al., 2015; Lebel et al., 2012; Sullivan et al., 2001; van Velsen et al., 2013; Vermeer et al., 2002). In the last 15 years, more and more longitudinal studies have been performed to estimate the rate of brain changes in aging or investigating possible causes and effects of these changes (Barrick et al., 2010; Discroll, 2009; de Groot et al., 2016; Du, 2006; Fjell et al., 2013, 2015; Fraser et al., 2015; Narvacan et al., 2017; Pfefferbaum et al., 2013; Raz et al., 2005, 2010; Sexton et al., 2014; Storsve et al., 2014; Sullivan et al., 2010). Overall, these studies show that the vulnerability of the brain to aging is heterogeneous. Furthermore, some studies show sex differences in the effect of age on the imaging markers (Fjell et al., 2015; Narvacan et al., 2017; Pfefferbaum et al., 2013; Raz et al., 2005), whereas others do not (Fjell et al., 2015; Raz et al., 2005).

Against the background, we aimed to comprise these different aspects in brain aging, by performing a comprehensive longitudinal assessment of brain aging in a middle- and old-aged population. We examined trajectories of volumetric, microstructural, and focal MRI markers in aging across a wide age range (45–95 years) in men and women based on a large prospective population-based cohort study with over 10,000 MRI scans. Furthermore, we analyzed the sequence in which MRI markers change in aging, so as to provide an overview of the concurrency of the changing imaging markers.

2. Methods and materials

2.1. Study population

This study is embedded within the Rotterdam Study, an ongoing prospective population-based study designed to investigate causes and consequences of age-related diseases. The design of the Rotterdam Study has been described previously (Ikram et al., 2017). Since 2005, brain MRI was implemented in the core Rotterdam Study protocol, and participants are invited every 3–4 years for repeat imaging. In Fig. 1, a flowchart of the inclusion of the MRI scans is shown. In this study, all available MRI scans from the Rotterdam Study that were acquired since August 2005 (date of installment of the MRI scanner in the research center) were included (n = 12,023 scans). Scans from participants with dementia or Parkinson's disease that were performed after clinical diagnosis were excluded (n = 110 MRI scans from 94 participants). Scans from participants with a symptomatic stroke that were performed after the event were excluded (n = 385 scans from 235 participants). Furthermore, MRI scans with incomplete acquisition, scans with artifacts hampering automated processing, unreliable tissue segmentation (or unreliable intracranial volume segmentation in case for the focal marker analysis), and incomplete ratings of microbleeds, cortical, and lacunar infarcts were excluded (volumetric and

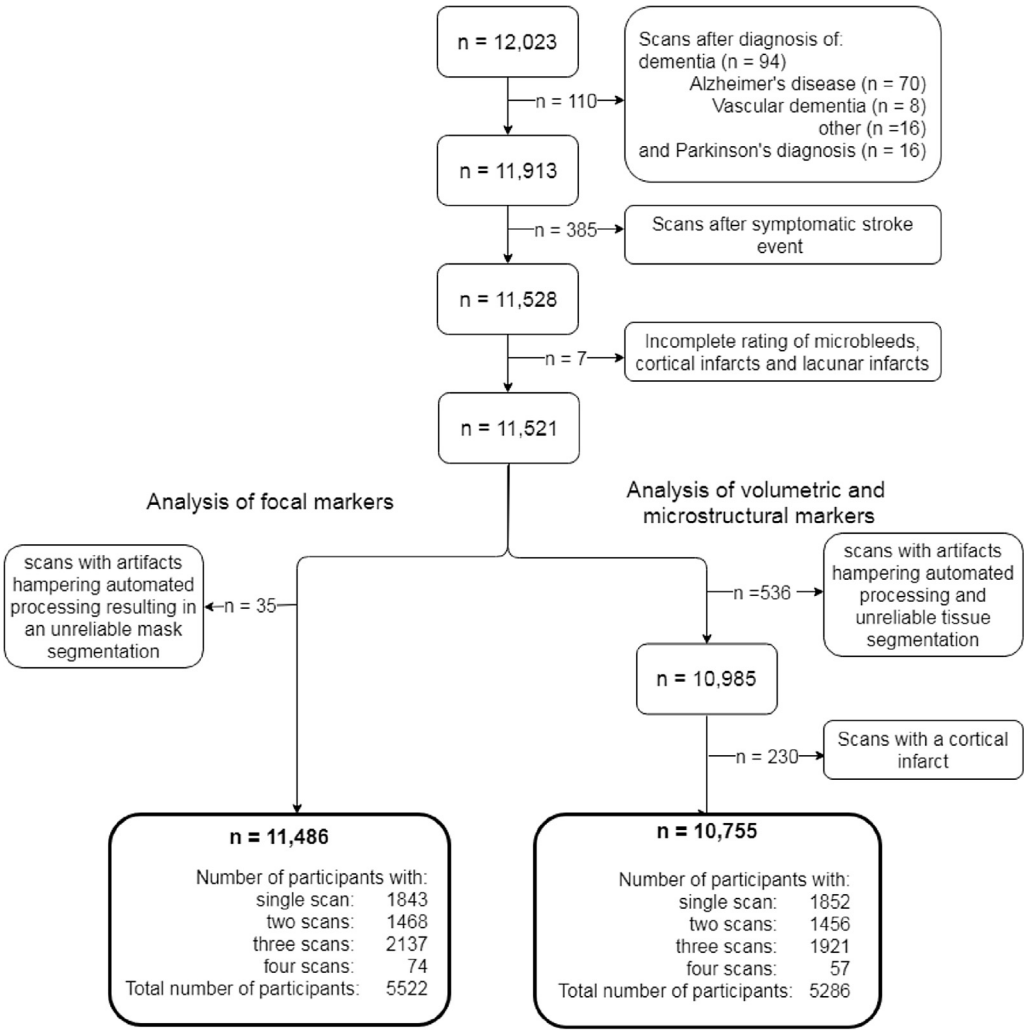

Fig. 1. A flowchart of the inclusion of MRI scans for both the analysis of volumetric and microstructural markers and the analysis of focal markers is shown. Abbreviation: MRI, magnetic resonance imaging.

microstructural markers analysis: n = 543 MRI scans, 4.7%; focal markers analysis: n = 42, 0.4%). Finally, all scans with MRI-defined cortical infarcts were excluded from volumetric and microstructural analysis (n = 230 MRI scans), but not for the focal marker analysis. In total, 10,755 MRI scans from 5286 participants were available for analysis of the volumetric and microstructural imaging markers, and 11,486 MRI scans from 5522 participants were available for analysis of focal markers.

2.2. MRI acquisition and processing

Brain MRI scanning was performed in all participants during the entire study period on the same single 1.5-Tesla MRI scanner (GE Signa Excite; GE Healthcare, Milwaukee, USA), keeping hardware and software setup unchanged over the entire study period. The scan protocol and sequence details have been described elsewhere (Ikram et al., 2015).

For brain volumetry, T1-weighted (voxel size 0.49 × 0.49 × 1.6 mm^3), proton density–weighted (voxel size 0.6 × 0.98 × 1.6 mm^3), and the fluid-attenuated inversion recovery (FLAIR) (voxel size 0.78 × 1.12 × 2.5 mm^3) scans were used for automated segmentation of supratentorial gray matter, white matter, cerebrospinal fluid (CSF), and white matter lesions (de Boer et al., 2009; Vrooman et al., 2007). All scans were transformed to the high-resolution data set (256 × 256 × 128) using tri-linear interpolation. Automated processing tools from the Brain Imaging Center, Montreal Neurological Institute and McGill University (www.bic.mni.mcgill.ca) were used to coregister the MRI data (based on mutual information) and subsequently normalize the intensities for each feature image volume using N3 (Sled et al., 1998). All segmentations were visually inspected and manually corrected if needed. Total brain volume was the sum of gray matter, normal-appearing white matter, and white matter lesion volume. Supratentorial intracranial volume was estimated by summing gray and white matter (consisting of the sum of normal-appearing white matter and white matter lesion volume) and CSF volumes (de Boer et al., 2009). For measurement of lobar volumes, an atlas was created in which the lobes were labeled according to a slightly modified version of the segmentation protocol, as described by Bokde et al. (Bokde et al., 2005; Ikram et al., 2008a). Subsequently, nonrigid transformation was used to transform this atlas to each brain as described previously (Ikram et al., 2008a), to obtain volume for each lobe. Furthermore, T1-weighted MR images were processed using FreeSurfer (Fischl et al., 2004) (version 5.1) to obtain cortical parcellations (n = 33) and subcortical structure volume of the hippocampus, putamen, amygdala, pallidum, and caudate nucleus.

For microstructural measures, diffusion tensor imaging (voxel size 3.3 × 2.2 × 3.5 mm^3) was used. A single shot, diffusion-weighted spin echo echo-planar imaging sequence was performed with maximum b value of 1000 s/mm^2 in 25 noncollinear directions; 3 b_0 volumes were acquired without diffusion weighting. Diffusion data were preprocessed using a standardized processing pipeline (Koppelmans et al., 2014), yielding (in combination with the tissue segmentation) global mean fractional anisotropy and mean diffusivity (MD) in the normal-appearing white matter (voxels of white matter excluding white matter lesions).

For (dichotomous) focal lesions, infarcts showing involvement of cortical gray matter were classified as cortical infarcts. Lacunar infarcts were defined by focal loss of noncortical tissue (size ≥ 3 and <15 mm) with signal intensity similar to CSF on all sequences, and when located supratentorially with a hyperintense rim on the FLAIR sequence (Vernooij et al., 2007). To differentiate lacunar infarcts from dilated perivascular spaces, symmetry of the lesions, sharp demarcation, and absence of a hyperintense rim on the FLAIR sequence supported presence of a dilated perivascular space (Adams et al., 2013). Cerebral microbleeds were rated on a 3-dimensional, T2*-weighted gradient-recalled echo MRI scan (voxel size 0.78 × 1.12 × 1.6 mm^3) as focal areas of very low signal intensity (Ikram et al., 2015). Note that although white matter lesions can be considered focal markers as well, we measured these continuously in the present study, and therefore for the purpose of visualization and comparison with other volumetric markers, we categorized white matter lesion volume as a volumetric marker.

2.3. Statistical analysis

Trajectories of global and lobar volumetric, cortical thickness, cortical volume and subcortical structure volume MRI markers, and microstructural measures were assessed using linear mixed models with random intercepts and slopes. Cortical and subcortical structure volumes and cortical thickness was the average of the left and right hemisphere. The global volumetric, microstructural, and subcortical structure volume markers that were modeled were white matter volume, white matter lesion volume, normal-appearing white matter volume, gray matter volume, CSF volume, total brain volume, hippocampus, putamen, amygdala, pallidum, and caudate nucleus volume, global fractional anisotropy, and global MD. The linear mixed models were performed using the "lme" function from the R-package "*nlme*" (Pinheiro et al., 2013). In each model, age of the participant at each measurement was used as the time variable. To account for possible nonlinear trajectories, exploratory analysis was performed to assess whether splines of age (with increasing degrees of freedom) improved the model compared with the linear age term. As a result from these analyses, splines of age with 1 knot were used in all models. Other covariates in the model were intracranial volume and sex. The interaction of sex and the spline coefficients of age was integrated into the model to test for possible slope differences between men and women. White matter lesion volume was natural log-transformed to account for the skewness of the measure distribution.

Next, trajectories of global and lobar volumetric, hippocampus volume, and microstructural MRI markers were Z-transformed to compare the temporal course of MRI marker change in aging. We selected these MRI markers for this analysis as these are currently the most extensively studied in aging and neurodegeneration, with relevant clinical interpretation. The transformation from absolute values to Z-scores was performed by subtracting the predicted curve value at age 45 years from the predicted curve at a certain age and dividing it by the standard deviation of the residuals of the linear mixed model. In case of an increasing trajectory (e.g., in white matter lesion volume), the Z-score trajectory was multiplied with −1 to orient all trajectories to the same direction as those of markers that decrease with age. The sequence with which imaging markers change in aging after age 45 years was determined by calculating the age at which a −2SD change compared with the mean population value at age 45 years was reached (Z-score of −2). We assessed the sequence of change for men and women separately.

For focal lesions, the probability of having one or more microbleeds, cortical infarcts, or lacunar infarcts was assessed using generalized estimating equations (GEEs). The GEE was performed using the "geeglm" function from the R-package "geepack" (HÃ¸jsgaard et al., 2006). In the GEE, natural cubic splines of age with 1 knot were used as the time variable. The covariates in the model were the same as in the linear mixed model, namely intracranial volume, gender, and the interaction of the splines of age and gender.

As sensitivity analysis, all analyses were performed after exclusion of scans before dementia and Parkinson's diagnosis and scans before a stroke event to investigate the effect of including preclinical scans. Furthermore, all analysis were performed after exclusion of participants with only a single MRI scan, to investigate the effect of possible population differences between participants with a single scan and those with multiple scans.

3. Results

Characteristics at first MRI scan of the participants included for studying the volumetric and microstructural markers and the focal markers are presented in Table 1. In Supplemental Table 1, the presence of several cardiovascular risk factors in our study population is shown. For studying the volumetric and microstructural markers, 5286 participants were included. The mean age at first scan was 64.4 years (range 45.7–97.9 years), and 2962 (56.0%) participants were women. The mean intracranial volume was 1138.2 mL (range 813.6–1699.4 mL). Of 5286 participants, 1852 participants had a single brain MRI scan, 1456 participants had 2 MRI scans, 1921 participants had 3 MRI scans, and 57 participants had 4 MRI scans available for analysis. The average follow-up time was 5.2 years (range 0.3–9.8). The mean scan interval between the first and second, second and third, and third and fourth MRI scan was, respectively, 4.0 (0.66), 1.9 (0.71), and 4.4 years (0.18). For studying the focal markers, 5522 participants were included. Of these 5522 participants, 1055, 375, and 144 participants had, respectively, one or more microbleeds, lacunar infarcts, and cortical infarcts at their first scan.

3.1. Trajectories of global volumetric and microstructural markers

Fig. 2 depicts the estimated trajectories of global volumetric, microstructural, and subcortical volume markers, for men and women separately. Furthermore, Supplemental Table 2 shows the trajectory values corresponding to the trajectories at age 45 and 95 years. White matter volume, normal-appearing white matter volume, gray matter volume, total brain volume, global fractional anisotropy, hippocampus volume, amygdala volume, and pallidum volume all showed a nonlinear decrease with age, whereas white matter lesion volume, CSF volume, and global MD increased (nonlinearly) with age. After approximately age 50–55 years, most trajectories showed an accelerated change, which was most pronounced for total brain volume, CSF volume, hippocampus volume, and MD (Fig. 2). Gray matter volume and putamen volume showed a more linear decrease with age compared with the other imaging markers. Caudate nucleus volume shows a more U-shaped curve with an increasing volume at increasing age, with the deflection point around age 65 years.

In Fig. 3A and B, the trajectories of the MRI markers are shown in Z-scores for men and women separately. In Supplemental Table 2, the corresponding Z-values at age 45 and 95 years are given. For both sexes, CSF and total brain volume reached the largest total change in Z-score (men −6.1; women −4.8), compared with the other MRI markers. There was significant interaction between age and sex for all markers, except for global FA, global MD, and amygdala volume (*p*-values of the age and sex interaction is given in Supplemental Table 2). In general, the trajectories show an earlier acceleration of changing markers in men compared with women (Fig. 3C).

3.2. Lobe-specific trajectories of volumetric markers and cortical parcellations

The lobe-specific trajectories of volumetric markers for men and women are shown in Supplemental Fig. 2 (absolute values) and Supplemental Fig. 3 (Z-scores). After taking into account differences in intracranial volume, the frontal lobe showed the largest relative change in each of the MRI markers, except for gray matter volume in men, where temporal gray matter showed the largest relative change. The occipital lobe showed the smallest change in each of the MRI markers, except for gray matter volume and for total lobar volume in women, where the parietal lobe showed the smallest relative change.

For all volumetric markers of the lobes, there was a significant interaction between age and sex, except for the log-transformed white matter lesion volume in the frontal, temporal, and occipital lobe, and gray matter volume in the occipital lobe. Similar to the trajectories of the MRI markers in the whole brain, the lobe-specific biomarkers in men showed earlier changing markers compared with women. In addition, the change expressed in Z-score was larger in men compared with women, except for white matter lesion volume.

Table 1
Characteristics of the study population

Characteristic	Analysis of volumetric and microstructural markers (N = 5286)	Analysis of focal markers (N = 5522)
Age at first scan, y	64.4 (10.7)	64.6 (10.8)
Age in men, y	64.2 (10.5)	64.4 (10.6)
Age in women, y	64.6 (10.8)	64.8 (10.9)
Sex, women	2962 (56.0)	3079 (55.8)
Intracranial volume, mL	1138.2 (115.7)	1138.4 (116.5)
Scan interval,y	3.3 (1.2)	3.3 (1.2)
Follow-up time, y	5.2 (1.1)	5.2 (1.0)
Availability of MRI scans with acceptable segmentation		
Number of participants with a single MRI scan	1852 (35.0)	1843 (33.4)
Number of participants with 2 MRI scans	1456 (27.5)	1468 (26.6)
Number of participants with 3 MRI scans	1921 (36.3)	2137 (38.7)
Number of participants with 4 MRI scans	57 (1.1)	74 (1.3)
Number of available MRI scans with acceptable segmentation	10,755	11,486
Baseline global FA[a]	0.34 (0.015)	
Baseline global MD, 10^{-3} mm^2/s[a]	0.74 (0.029)	
Baseline total white matter volume, mL	407.3 (59.8)	
Baseline normal-appearing white matter volume, mL	401.3 (61.3)	
Baseline white matter lesion volume[b], mL	2.9 (1.6–6.0)	
Baseline gray matter volume, mL	529.7 (54.9)	
Baseline cerebrospinal fluid volume, mL	198.9 (54.9)	
Baseline total brain volume, mL	937.0 (100.1)	
Baseline hippocampus volume[a], mL	3.9 (0.52)	
Baseline putamen volume[a], mL	4.6 (0.61)	
Baseline amygdala volume[a], mL	1.4 (0.19)	
Baseline pallidum volume[a], mL	1.5 (0.23)	
Baseline caudate nucleus volume[a], mL	3.4 (0.52)	
Microbleed(s) at baseline scan	1003 (19.0)	1055 (19.1)
Lacunar infarct(s) at baseline scan	336 (6.4)	375 (6.8)
Cortical infarct(s) at baseline scan	Not applicable	144 (2.6)

Continuous variables are presented as means (standard deviations) and categorical variables as number (percentages).
Key: FA, fractional anisotropy; MD, mean diffusivity; MRI, magnetic resonance imaging; N, number of participants; sec, seconds.
[a] Data on the subcortical structure volumes were the average of the left and right volume. Subcortical structure volume was missing in 23 participants due to failed FreeSurfer segmentation. Data on global FA and global MD in the normal-appearing white matter were missing in 295 participants, due to failed segmentation of the diffusion tensor images.
[b] White matter lesion volume are presented as median (interquartile range).

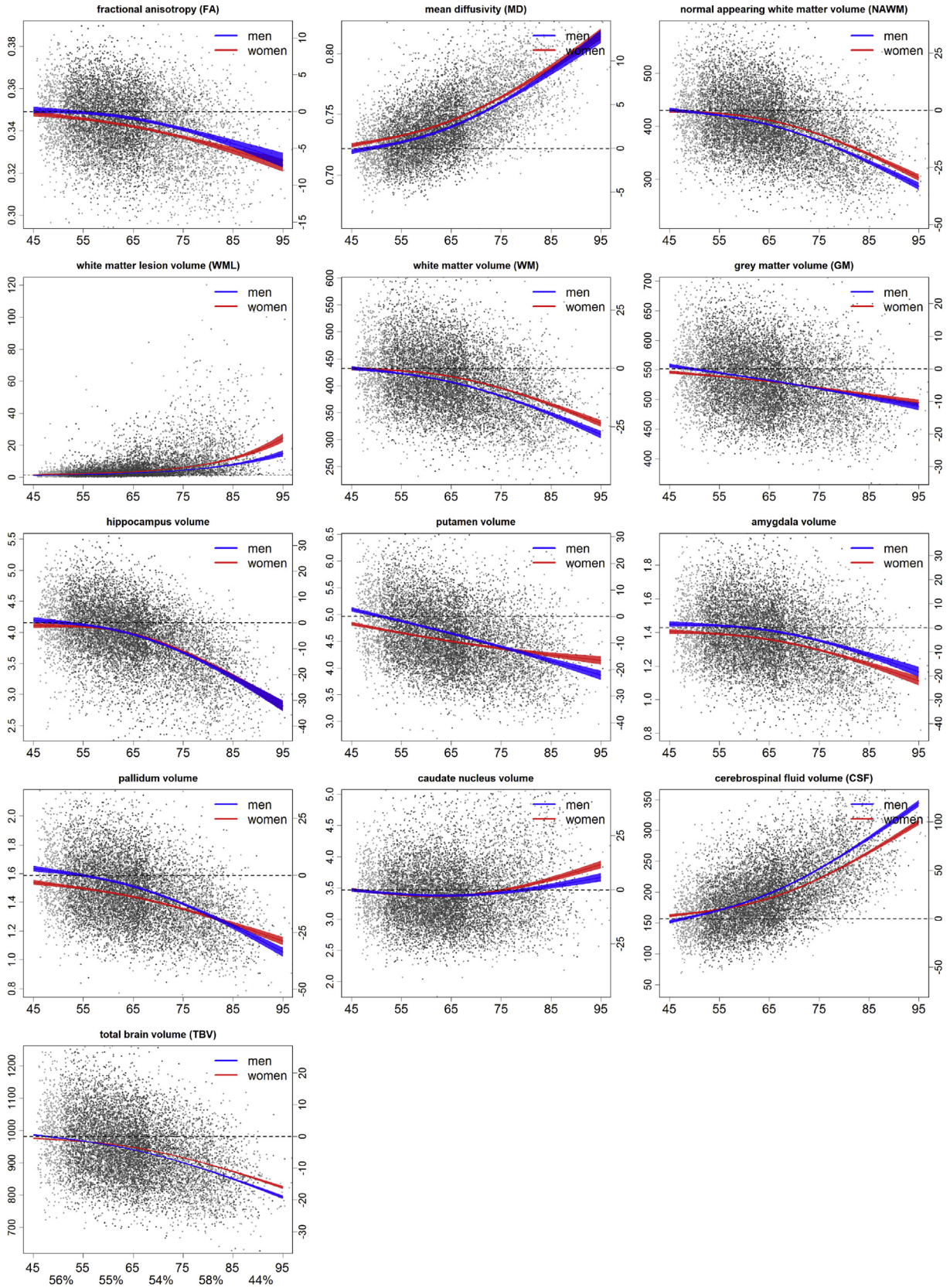

Fig. 2. Trajectories of each MRI marker of interest for men and women. In blue and red, the average trajectory of, respectively, men and women are shown with corresponding confidence interval. The x-axis represents the age at time of the scan, the left y-axis represents the absolute marker value, the right y-axis the percentage of change compared with baseline, where baseline is the average value at age 45 years of men and women. The log-transformed white matter lesion trajectory was back-transformed to obtain the white matter lesion volume trajectory. Because the nontransformed trajectory of white matter lesion volume is shown, only the absolute marker values on the left axis are presented. In the background of the graphs, scatterplots of all measurements are shown. Measurements from the same participant are shown in 3 shades of gray, where the light gray, darker gray, and darkest gray scatter points are, respectively, the first, second, and third measurement. Below the x-axis in the graph of total brain volume, the proportion scans from women are shown for each 10-year age bin. Abbreviation: MRI, magnetic resonance imaging. (For interpretation of the references to color in this figure legend, the reader is referred to the Web version of this article.)

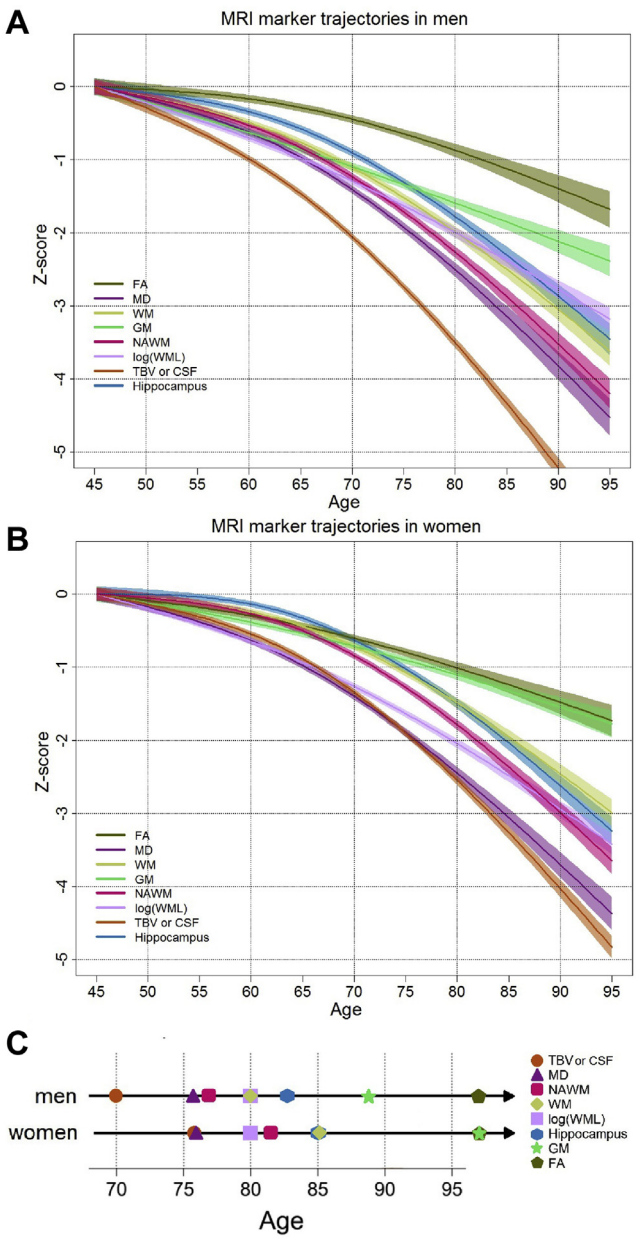

Fig. 3. Trajectories of change in Z-score for each MRI marker of interest (with corresponding confidence interval) for (A) men and (B) women. (C) Representation of the age at which Z-score of each MRI marker reached a 2SD change compared with the value at age 45 years. Trajectories are shown for global FA, global MD, WM, GM volume, NAWM, natural log transform of white matter lesion volume (log [WML]), TBV, CSF volume, and hippocampus volume (Hippocampus). The trajectories of MRI markers which increase with age were multiplied with −1 to orient all lines in the same direction. The trajectory of CSF and total brain volume overlap; therefore, this trajectory represents both TBV and CSF multiplied with −1. In men the age at which a 2SD change occurred is the same for white matter and the natural log transform of white matter lesion; therefore, at age 80 years the symbols for these two markers are overlapping. The same holds for fractional anisotropy and gray matter volume in women. Abbreviations: CSF, cerebrospinal fluid; FA, fractional anisotropy; GM, gray matter; MD, mean diffusivity; MRI, magnetic resonance imaging; NAWM, normal-appearing white matter volume; TBV, total brain volume; WM, white matter volume. (For interpretation of the references to color in this figure legend, the reader is referred to the Web version of this article.)

The trajectories of the volume and thickness of the cortical parcellations in men and women are shown in Supplemental Figs. 3–6. These figures show a mix of more linear and nonlinear trajectories, either increasing, decreasing, or stable over age for the volume and thickness of cortical parcellations. Differences between men and women are visible in several parcellations; however, the direction of these differences is mixed, where in some parcellations, there seems to be only an intercept difference, and in other parcellations, men show an earlier decrease in volume or thickness and vice versa. Overall, the amount of change in cortical volume was different across and within lobes, were certain regions in the frontal, temporal, and parietal lobe decreased ~25% at age 95 years compared with age 45 years, whereas other regions showed less vulnerability to age.

3.3. Sequence of changing volumetric and microstructural MRI markers

The sequence in which volumetric and microstructural MRI markers reach a 2SD change after age 45 years is shown in Fig. 3C. For both men and women, total brain volume and global MD were the first 2 markers to change after age 45 years, although in men, changes started 6 years before women (70 years vs. 76 years). Other differences between men and women are primarily a later change in women of normal-appearing white matter volume and normal-appearing white matter volume (Fig. 3C). Global gray matter volume change occurs relatively late in both sexes, with the largest age difference between men and women (89 in men, 97 in women). The last marker in the sequence was global fractional anisotropy, occurring at approximately the same age in both sexes (age 97 years). The sequence of reaching a 2SD change after age 45 years of total lobe volume is shown in Supplemental Fig. 2A. The first lobe that changes after age 45 years is the frontal lobe, which is then followed by the temporal lobe. There is a difference in sequence between sexes, where in men, after the temporal lobe, the parietal lobe changes and finally the occipital lobe, whereas in women, this is the other way around. Overall, the changes in total lobe volume of the frontal, temporal, parietal, and occipital lobe occurs, respectively, 6, 7, 11, and 4 years later in women.

3.4. Focal imaging markers in aging

Fig. 4 shows the probability curves in aging for microbleeds, cortical infarcts, and lacunar infarcts on MRI, for men and women

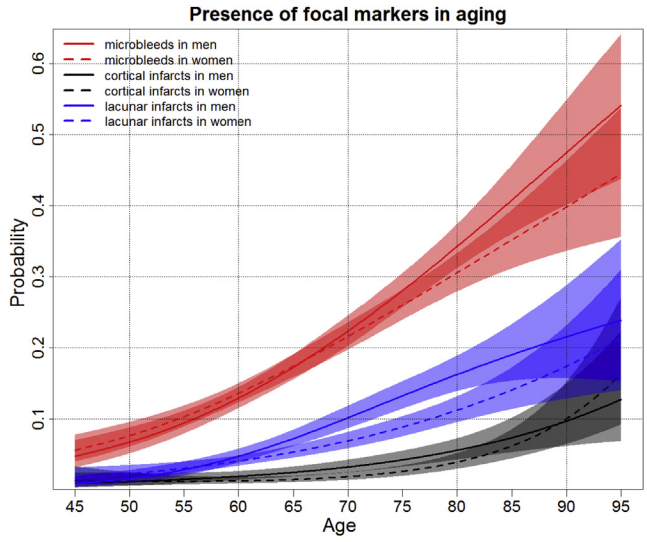

Fig. 4. Probability curves of the presence of the focal markers: one or more microbleeds, cortical infarct, or lacunar infarct in men and women in aging. The solid and dotted lines represent the trajectories of, respectively, men and women with corresponding 95% confidence interval. The red, black, and blue prediction lines represent the probability of presence of respectively one or more microbleeds, cortical infarct, and lacunar infarct. (For interpretation of the references to color in this figure legend, the reader is referred to the Web version of this article.)

separately. The probability of having one or more microbleeds ranged from 4.7% (age 45 years) to 54.8% (age 95 years) and was overall higher than lacunar infarcts (0.9%–23.8%, respectively) and cortical infarcts (1.0%–15.2%, respectively). Men had higher prevalence of lacunar infarcts and cortical infarcts than women, respectively, for the ages 64.7 to 83.7 years, and 54.9 to 90.7 years. The interaction between age and sex was not significant in any of the focal markers.

3.5. Sensitivity analyses

We performed a sensitivity analysis in which scans before a dementia or Parkinson's diagnosis, or scans before a stroke event were excluded (n = 488 scans). Furthermore, we performed a sensitivity analysis in which only participants with multiple scans were included. Both sensitivity analyses showed similar results compared with the original results.

4. Discussion

In this study, we present a comprehensive longitudinal assessment of brain aging, providing an overview of the concurrency of changing imaging markers. We show trajectories of volumetric, microstructural, and focal imaging markers in a large aging population, based on longitudinal MRI data. The trajectories of the different global, cortical, subcortical, and lobar MRI markers follow a nonlinear curve, with accelerating change with advancing age. Regarding temporal patterns, the change in MRI markers generally occurs earlier in men than in women. Among focal lesions, microbleeds show the highest prevalence and steepest increase across the age range, up to 54.8% in age 95 years. Overall, men tend to have higher prevalence of focal lesions (microbleeds, lacunes, and cortical infarcts) compared with women.

A major strength of this study is its longitudinal design, which increases sensitivity to detect rates of change compared with a more often used cross-sectional design. In combination with the large sample size from a population-based setting, this increases the generalizability of our results. Furthermore, because of the availability of many different MRI markers within this large longitudinal sample, we were able to simultaneously analyze and compare the aging effect of these markers. However, some limitations also need to be considered. Owing to a relatively short time between the first and last scan of participants, and relatively sparse proportion of older participants, the estimated trajectories may not be representing the longitudinal effect at the older ages reliably. Furthermore, although scans from participants after diagnosis of Alzheimer's disease, Parkinson's disease, and stroke were excluded, it is likely that a proportion of the participants are prodromal, which could influence the trajectories. However, our sensitivity analysis in which we also excluded scans before diagnosis showed similar results. Therefore, we believe that the effect of prodromal participants on these trajectories is minimal. Another limitation of this study is the possible selection bias, due to differences in people participating in the scan study and participants that refuse (Poels et al., 2011). Furthermore, the same could hold for participants with only a single scan compared with participants with multiple scans. In 35.0% of the participants, there was only one MRI scan available for analysis. An important advantage of including persons with both single and multiple brain scans is that we include all available information and avoid the risk of including relatively healthier survivors with only longitudinal information. However, in this study, results remained similar after excluding participants with only a single scan.

The trajectories of whole brain, cortical, subcortical, and lobar volumetric markers we assessed are largely in accordance with previous literature (Coupe et al., 2017; DeCarli et al., 2005; Lockhart and DeCarli, 2014; Narvacan et al., 2017; Storsve et al., 2014). Our study confirms previous findings that showed that white matter volume changes in aging are nonlinear, with a more rapid change with advancing age, whereas gray matter shows a smaller and more linear decrease with advancing age (DeCarli et al., 2005; Fjell et al., 2013; Fotenos et al., 2005; Ge et al., 2002; Raz et al., 2005). Previous studies have shown different curves for subcortical structures, for example, hippocampus volume atrophy accelerates at increasing age, whereas the caudate nucleus follows a more stable curve with increasing age (Coupe et al., 2017; Fjell et al., 2013); our study also shows a nonlinear decrease in volume for hippocampus, amygdala, and pallidum in aging and a more linear volume decrease in putamen volume and a U-shaped curve for the caudate nucleus volume.

Our study adds to existing literature in showing the longitudinal trajectories of microstructural white matter changes on top of these macrostructural changes. As understanding normal aging is essential to better understand or detect abnormal aging, we examined the sequence with which these imaging markers change with age and found among volumetric markers total brain volume to change first, which is likely due to the fact that this reflects a summation of changes in other tissues as well. This was followed by total white matter, with total gray matter being one of the last markers to change. An important limitation of our method determining the sequence is that it depends on the amount of change relative to the variation, meaning that differences in variation and measurement error directly influences the sequence. In accordance with literature, lobar trajectories of volumetric imaging markers and cortical volume and thickness in this study confirm regional differences in the amount of atrophy within and across lobes (Fjell and Walhovd, 2010; Fjell et al., 2014; Lockhart and DeCarli, 2014). Trajectories of white matter and total lobe volume show that the frontal lobe is most affected, which has also been described in other studies (DeCarli et al., 2005; Discroll, 2009; Raz et al., 2005; Sullivan and Pfefferbaum, 2007). Furthermore, our study shows that within frontal, temporal, and parietal lobe, there are certain cortical regions highly affected by aging, reaching up to ~25% decrease in volume at age 95 years compared with age 45 years. In addition, we determined the sequence with which the lobes change with age, showing that total frontal lobe volume changes first, followed by the temporal lobe, parietal lobe, and lastly the occipital lobe. Several hypotheses have been proposed to explain this selective vulnerability of the brain regions, including the "retrogenesis hypothesis" which states that late maturing regions are most vulnerable to aging and the hypothesis of an anterior-to-posterior gradient of age vulnerability. However, the underlying biological mechanism remains unknown (Fjell et al., 2014; Raz et al., 1997).

Although several studies have looked at sex differences in volumetric imaging markers in the aging brain, they have not yielded consistent results. Some studies showed that women have overall a proportionally larger gray matter volume and less white matter volume than men (Ikram et al., 2008b; Leonard et al., 2008), whereas others showed the opposite (Ge et al., 2002; Good et al., 2001). A recent cross-sectional study showed absolute volume differences between men and women for several markers, but the shape of the trajectories across the life span was equal between men and women (Narvacan et al., 2017). Discrepancies in these findings could most likely be explained by cross-sectional study design, small sample sizes and limited spread of the MRI data over the total age range. In this large longitudinal study, we show sex differences in the trajectories of all volumetric MRI markers in normal aging, after correcting for head size differences. We show an earlier acceleration and a larger amount of change in men compared with women for both whole brain, subcortical, cortical,

and lobar volumes, but also for focal lesions. These differences are also reflected in a difference in the sequence in which imaging markers change between men and women, where especially total brain volume, white matter, normal-appearing white matter, and gray matter volume changes in women appear later in the sequence than in men. These sex-specific differences are important to take into account when normative reference values on a lobar level, for example, in a memory clinic, would be applied in a clinical setting to assess pathology in individual patients.

Less is known on global microstructural changes in aging, but the microstructural MRI trajectories we describe are in accordance with published literature, in which decreased global fractional anisotropy and increased global MD with age have been suggested to reflect a reduced microstructural integrity (Beaulieu, 2002). Our results suggest global MD to be a more sensitive marker of reduced microstructural organization in aging, as it showed an earlier and more accelerated change in comparison with global fractional anisotropy. In fact, we found that global MD was the second marker to change (after total brain volume) in the sequence of changing MRI markers, before change in volumetric white matter markers, indicating that microstructural changes precede volumetric white matter changes. This is in agreement with a previous study by our group showing that microstructural changes in white matter appear before development of white matter lesions (de Groot et al., 2013).

Similar to volumetric and microstructural MRI markers, focal markers also show a nonlinear relationship with age. The probability of having one or more microbleeds was higher than having ischemic lesions (lacunes and cortical infarcts) at all ages. Over practically the entire age range, the probability of having one or more lacunar infarcts (up to 23.8%) was higher than for cortical infarcts (maximum 15.2%). This corresponds to a previous study from our own group, which showed in a cross-sectional sample of the same study population that prevalence of microbleeds is higher than infarcts, and that the prevalence of lacunar infarcts is higher than cortical infarcts (Poels et al., 2010). Age trajectories for these focal lesions, especially derived from longitudinal data, were lacking so far, and the present study provides important information that may also be useful as a background in a clinical setting. The overall prevalence of cortical and lacunar infarcts is comparable with the prevalence of silent infarcts in the different age categories described in a previous cross-sectional study in Rotterdam Study participants (not included in the present sample) (Vermeer et al., 2007).

Between the age range 65–85 years, the probability of having one or more lacunar and cortical infarcts was higher in men. This is in contrast to what previously has been shown in a study within other subjects from the same community-dwelling population, where the prevalence of silent infarcts was higher in women than in men (Vermeer et al., 2002), whereas in other studies no significant difference between the prevalence of infarcts were found between men and women (Vermeer et al., 2007). A possible reason for the differences of our results with other reports is that we made no distinction between silent and symptomatic infarcts, while it has been shown that the prevalence of symptomatic infarcts is higher in men (Goldstein et al., 2001). Another explanation of our contradictory findings could be the larger sample size in combination with a longitudinal design, which may be more sensitive to find gender differences.

In this study, we focused on aggregated measures derived from the images; however, data-driven methods using the complete scan information, such as machine learning, could provide new insights in the effect of aging. Another interesting next step is to assess the effect of different determinants on the aging trajectories.

Overall, the trajectories of imaging markers in brain aging that we describe are essential background information for studies into age-related neurological diseases, or for clinical translation, for example, use of reference values. Especially in studies looking at differences between age-related pathology and normal aging, it is important to take into account the nonlinear age effects we found for all markers, as well as the interaction of age and sex for several markers.

Disclosure statement

The authors have no actual or potential conflicts of interest.

Acknowledgements

This study is part of the EuroPOND initiative, which is funded by the European Union's Horizon 2020 research and innovation program under grant agreement No. 666992. This project has received funding from the European Research Council (ERC) under the European Union's Horizon 2020 research and innovation program (project: ORACLE, grant agreement No: 678543). The Rotterdam Study is funded by Erasmus Medical Center and Erasmus University, Rotterdam, the Netherlands Organization for the Health Research and Development (ZonMw), the Research Institute for Diseases in the Elderly (RIDE), the Ministry of Education, Culture and Science, the Ministry for Health, Welfare and Sports, the European Commission (DG XII), and the Municipality of Rotterdam.

Appendix A. Supplementary data

Supplementary data associated with this article can be found, in the online version, at https://doi.org/10.1016/j.neurobiolaging.2018.07.001.

References

Adams, H.H., Cavalieri, M., Verhaaren, B.F., Bos, D., van der Lugt, A., Enzinger, C., Vernooij, M.W., Schmidt, R., Ikram, M.A., 2013. Rating method for dilated Virchow-Robin spaces on magnetic resonance imaging. Stroke 44, 1732–1735.

Barrick, T.R., Charlton, R.A., Clark, C.A., Markus, H.S., 2010. White matter structural decline in normal ageing: a prospective longitudinal study using tract-based spatial statistics. Neuroimage 51, 565–577.

Beaulieu, C., 2002. The basis of anisotropic water diffusion in the nervous system - a technical review. NMR Biomed. 15, 435–455.

Bokde, A.L., Teipel, S.J., Schwarz, R., Leinsinger, G., Buerger, K., Moeller, T., Moller, H.J., Hampel, H., 2005. Reliable manual segmentation of the frontal, parietal, temporal, and occipital lobes on magnetic resonance images of healthy subjects. Brain Res. Brain Res. Protoc. 14, 135–145.

Coffey, C.E., Lucke, J.F., Saxton, J.A., Ratcliff, G., Unitas, L.J., Billig, B., Bryan, R.N., 1998. Sex differences in brain aging: a quantitative magnetic resonance imaging study. Arch. Neurol. 55, 169–179.

Coupe, P., Catheline, G., Lanuza, E., Manjon, J.V., Alzheimer's Disease Neuroimaging I, 2017. Towards a unified analysis of brain maturation and aging across the entire lifespan: a MRI analysis. Hum. Brain Mapp. 38, 5501–5518.

Cox, S.R., Ritchie, S.J., Tucker-Drob, E.M., Liewald, D.C., Hagenaars, S.P., Davies, G., Wardlaw, J.M., Gale, C.R., Bastin, M.E., Deary, I.J., 2016. Ageing and brain white matter structure in 3,513 UK Biobank participants. Nat. Commun. 7, 13629.

de Boer, R., Vrooman, H.A., van der Lijn, F., Vernooij, M.W., Ikram, M.A., van der Lugt, A., Breteler, M.M., Niessen, W.J., 2009. White matter lesion extension to automatic brain tissue segmentation on MRI. Neuroimage 45, 1151–1161.

de Groot, M., Verhaaren, B.F., de Boer, R., Klein, S., Hofman, A., van der Lugt, A., Ikram, M.A., Niessen, W.J., Vernooij, M.W., 2013. Changes in normal-appearing white matter precede development of white matter lesions. Stroke 44, 1037–1042.

de Groot, M., Ikram, M.A., Akoudad, S., Krestin, G.P., Hofman, A., van der Lugt, A., Niessen, W.J., Vernooij, M.W., 2015. Tract-specific white matter degeneration in aging: the Rotterdam Study. Alzheimers Dement 11, 321–330.

de Groot, M., Cremers, L.G., Ikram, M.A., Hofman, A., Krestin, G.P., van der Lugt, A., Niessen, W.J., Vernooij, M.W., 2016. White matter degeneration with aging: longitudinal diffusion MR imaging analysis. Radiology 279, 532–541.

DeCarli, C., Massaro, J., Harvey, D., Hald, J., Tullberg, M., Au, R., Beiser, A., D'Agostino, R., Wolf, P.A., 2005. Measures of brain morphology and infarction in the framingham heart study: establishing what is normal. Neurobiol. Aging 26, 491–510.

Discroll, I., 2009. Longitudinal pattern of regional brain volume change differentiates normal aging from MCI. Neurology 72, 1903–1913.
Du, A., 2006. Age effects on atrophy rates of entorhinal cortex and hippocampus. Neurobiol. Aging 27, 733–740.
Fischl, B., Salat, D.H., van der Kouwe, A.J., Makris, N., Segonne, F., Quinn, B.T., Dale, A.M., 2004. Sequence-independent segmentation of magnetic resonance images. Neuroimage 23 (Suppl 1), S69–S84.
Fjell, A.M., Walhovd, K.B., 2010. Structural brain changes in aging: courses, causes and cognitive consequences. Rev. Neurosci. 21, 187–221.
Fjell, A.M., Westlye, L.T., Grydeland, H., Amlien, I., Espeseth, T., Reinvang, I., Raz, N., Holland, D., Dale, A.M., Walhovd, K.B., Alzheimer Disease Neuroimaging I, 2013. Critical ages in the life course of the adult brain: nonlinear subcortical aging. Neurobiol. Aging 34, 2239–2247.
Fjell, A.M., McEvoy, L., Holland, D., Dale, A.M., Walhovd, K.B., Alzheimer's Disease Neuroimaging, I., 2014. What is normal in normal aging? Effects of aging, amyloid and Alzheimer's disease on the cerebral cortex and the hippocampus. Prog. Neurobiol. 117, 20–40.
Fjell, A.M., Grydeland, H., Krogsrud, S.K., Amlien, I., Rohani, D.A., Ferschmann, L., Storsve, A.B., Tamnes, C.K., Sala-Llonch, R., Due-Tønnessen, P., Bjørnerud, A., 2015. Development and aging of cortical thickness correspond to genetic organization patterns. Proc. Natl. Acad. Sci. U. S. A. 112, 15462–15467.
Fotenos, A.F., Snyder, A.Z., Girton, L.E., Morris, J.C., Buckner, R.L., 2005. Normative estimates of cross-sectional and longitudinal brain volume decline in aging and AD. Neurology 64, 1032–1039.
Fraser, M.A., Shaw, M.E., Cherbuin, N., 2015. A systematic review and meta-analysis of longitudinal hippocampal atrophy in healthy human ageing. Neuroimage 112, 364–374.
Ge, Y., Grossman, R.I., Babb, J.S., Rabin, M.L., Mannon, L.J., Kolson, D.L., 2002. Age-related total gray matter and white matter changes in normal adult brain. Part I: volumetric MR imaging analysis. AJNR Am. J. Neuroradiol. 23, 1327–1333.
Goldstein, L.B., Adams, R., Becker, K., Furberg, C.D., Gorelick, P.B., Hademenos, G., Hill, M., Howard, G., Howard, V.J., Jacobs, B., Levine, S.R., Mosca, L., Sacco, R.L., Sherman, D.G., Wolf, P.A., del Zoppo, G.J., 2001. Primary prevention of ischemic stroke: a statement for healthcare professionals from the Stroke Council of the American Heart Association. Stroke 32, 280–299.
Good, C.D., Johnsrude, I.S., Ashburner, J., Henson, R.N., Friston, K.J., Frackowiak, R.S., 2001. A voxel-based morphometric study of ageing in 465 normal adult human brains. Neuroimage 14, 21–36.
Gur, R.C., Mozley, P.D., Resnick, S.M., Gottlieb, G.L., Kohn, M., Zimmerman, R., Herman, G., Atlas, S., Grossman, R., Berretta, D., 1991. Gender differences in age effect on brain atrophy measured by magnetic resonance imaging. Proc. Natl. Acad. Sci. U S A. 88, 2845–2849.
HÃjsgaard, S., Halekoh, U., Yan, J., 2006. The R package geepack for generalized estimating equations. J. Stat. Softw. 15, 1–11.
Ikram, M.A., Vernooij, M.W., Hofman, A., Niessen, W.J., van der Lugt, A., Breteler, M.M., 2008a. Kidney function is related to cerebral small vessel disease. Stroke 39, 55–61.
Ikram, M.A., Vrooman, H.A., Vernooij, M.W., van der Lijn, F., Hofman, A., van der Lugt, A., Niessen, W.J., Breteler, M.M., 2008b. Brain tissue volumes in the general elderly population. The Rotterdam Scan Study. Neurobiol. Aging 29, 882–890.
Ikram, M.A., van der Lugt, A., Niessen, W.J., Koudstaal, P.J., Krestin, G.P., Hofman, A., Bos, D., Vernooij, M.W., 2015. The Rotterdam Scan Study: design update 2016 and main findings. Eur. J. Epidemiol. 30, 1299–1315.
Ikram, M.A., Brusselle, G.G.O., Murad, S.D., van Duijn, C.M., Franco, O.H., Goedegebure, A., Klaver, C.C.W., Nijsten, T.E.C., Peeters, R.P., Stricker, B.H., Tiemeier, H., Uitterlinden, A.G., Vernooij, M.W., Hofman, A., 2017. The Rotterdam Study: 2018 update on objectives, design and main results. Eur. J. Epidemiol. 32, 807–850.
Jernigan, T.L., Press, G.A., Hesselink, J.R., 1990. Methods for measuring brain morphologic features on magnetic resonance images. Validation and normal aging. Arch. Neurol. 47, 27–32.
Jernigan, T.L., Archibald, S.L., Berhow, M.T., Sowell, E.R., Foster, D.S., Hesselink, J.R., 1991. Cerebral structure on MRI, Part I: localization of age-related changes. Biol. Psychiatry 29, 55–67.
Koppelmans, V., de Groot, M., de Ruiter, M.B., Boogerd, W., Seynaeve, C., Vernooij, M.W., Niessen, W.J., Schagen, S.B., Breteler, M.M., 2014. Global and focal white matter integrity in breast cancer survivors 20 years after adjuvant chemotherapy. Hum. Brain Mapp. 35, 889–899.
Krishnan, K.R., Husain, M.M., McDonald, W.M., Doraiswamy, P.M., Figiel, G.S., Boyko, O.B., Ellinwood, E.H., Nemeroff, C.B., 1990. In vivo stereological assessment of caudate volume in man: effect of normal aging. Life Sci. 47, 1325–1329.
Lebel, C., Gee, M., Camicioli, R., Wieler, M., Martin, W., Beaulieu, C., 2012. Diffusion tensor imaging of white matter tract evolution over the lifespan. Neuroimage 60, 340–352.
Leonard, C.M., Towler, S., Welcome, S., Halderman, L.K., Otto, R., Eckert, M.A., Chiarello, C., 2008. Size matters: cerebral volume influences sex differences in neuroanatomy. Cereb. Cortex. 18, 2920–2931.
Lockhart, S.N., DeCarli, C., 2014. Structural imaging measures of brain aging. Neuropsychol. Rev. 24, 271–289.
Mu, Q., Xie, J., Wen, Z., Weng, Y., Shuyun, Z., 1999. A quantitative MR study of the hippocampal formation, the amygdala, and the temporal horn of the lateral ventricle in healthy subjects 40 to 90 years of age. AJNR Am. J. Neuroradiol. 20, 207–211.
Narvacan, K., Treit, S., Camicioli, R., Martin, W., Beaulieu, C., 2017. Evolution of deep gray matter volume across the human lifespan. Hum. Brain Mapp. 38, 3771–3790.
Pfefferbaum, A., Mathalon, D.H., Sullivan, E.V., Rawles, J.M., Zipursky, R.B., Lim, K.O., 1994. A quantitative magnetic resonance imaging study of changes in brain morphology. Arch. Neurol. 51, 874–887.
Pfefferbaum, A., Rohlfing, T., Rosenbloom, M.J., Chu, W., Colrain, I.M., Sullivan, E.V., 2013. Variation in longitudinal trajectories of regional brain volumes of healthy men and women (ages 10 to 85 years) measured with atlas-based parcellation of MRI. Neuroimage 65, 176–193.
Pinheiro, J., Bates, D., DebRoy, S., Sarkar, D., R Development Core Team, 2013. Nlme: Linear And Nonlinear Mixed Effects Models. R Package Version 3, pp. 1–108. https://CRAN.R-project.org/package=nlme.
Poels, M.M., Vernooij, M.W., Ikram, M.A., Hofman, A., Krestin, G.P., van der Lugt, A., Breteler, M.M., 2010. Prevalence and risk factors of cerebral microbleeds: an update of the Rotterdam scan study. Stroke 41, S103–S106.
Poels, M.M., Ikram, M.A., van der Lugt, A., Hofman, A., Krestin, G.P., Breteler, M.M., Vernooij, M.W., 2011. Incidence of cerebral microbleeds in the general population: the Rotterdam Scan Study. Stroke 42, 656–661.
Raz, N., Gunning, F.M., Head, D., Dupuis, J.H., McQuain, J., Briggs, S.D., Loken, W.J., TA, E., Acker, J.D., 1997. Selective aging of the human cerebral cortex observed in vivo: differential vulnerability of the prefrontal gray matter. Cereb. Cortex. 7, 268–282.
Raz, N., Lindenberger, U., Rodrigue, K.M., Kennedy, K.M., Head, D., Williamson, A., Dahle, C., Gerstorf, D., Acker, J.D., 2005. Regional brain changes in aging healthy adults: general trends, individual differences and modifiers. Cereb. Cortex. 15, 1676–1689.
Raz, N., Ghisletta, P., Rodrigue, K.M., Kennedy, K.M., Lindenberger, U., 2010. Trajectories of brain aging in middle-aged and older adults: regional and individual differences. Neuroimage 51, 501–511.
Sexton, C.E., Walhovd, K.B., Storsve, A.B., Tamnes, C.K., Westlye, L.T., Johansen-Berg, H., Fjell, A.M., 2014. Accelerated changes in white matter microstructure during aging: a longitudinal diffusion tensor imaging study. J. Neurosci. 34, 15425–15436.
Sled, J.G., Zijdenbos, A.P., Evans, A.C., 1998. A nonparametric method for automatic correction of intensity nonuniformity in MRI data. IEEE Trans. Med. Imaging 17, 87–97.
Storsve, A.B., Fjell, A.M., Tamnes, C.K., Westlye, L.T., Overbye, K., Aasland, H.W., Walhovd, K.B., 2014. Differential longitudinal changes in cortical thickness, surface area and volume across the adult life span: regions of accelerating and decelerating change. J. Neurosci. 34, 8488–8498.
Sullivan, E.V., Pfefferbaum, A., 2007. Neuroradiological characterization of normal adult ageing. Br. J. Radiol. 80, S99–S108.
Sullivan, E.V., Marsh, L., Mathalon, D.H., Lim, K.O., Pfefferbaum, A., 1995. Age-related decline in MRI volumes of temporal lobe gray matter but not hippocampus. Neurobiol. Aging 16, 591–606.
Sullivan, E.V., Adalsteinsson, E., Hedehus, M., Ju, C., Moseley, M., Lim, K.O., Pfefferbaum, A., 2001. Equivalent disruption of regional white matter microstructure in ageing healthy men and women. Neuroreport 12, 99–104.
Sullivan, E.V., Rohlfing, T., Pfefferbaum, A., 2010. Longitudinal study of callosal microstructure in the normal adult aging brain using quantitative DTI fiber tracking. Dev. Neuropsychol. 35, 233–256.
van Velsen, E.F., Vernooij, M.W., Vrooman, H.A., van der Lugt, A., Breteler, M.M., Hofman, A., Niessen, W.J., Ikram, M.A., 2013. Brain cortical thickness in the general elderly population: the Rotterdam Scan Study. Neurosci. Lett. 550, 189–194.
Vermeer, S.E., Koudstaal, P.J., Oudkerk, M., Hofman, A., Breteler, M.M., 2002. Prevalence and risk factors of silent brain infarcts in the population-based Rotterdam Scan Study. Stroke 33, 21–25.
Vermeer, S.E., Longstreth Jr., W.T., Koudstaal, P.J., 2007. Silent brain infarcts: a systematic review. Lancet Neurol. 6, 611–619.
Vernooij, M.W., Ikram, M.A., Tanghe, H.L., Vincent, A.J., Hofman, A., Krestin, G.P., Niessen, W.J., Breteler, M.M., van der Lugt, A., 2007. Incidental findings on brain MRI in the general population. N. Engl. J. Med. 357, 1821–1828.
Vrooman, H.A., Cocosco, C.A., van der Lijn, F., Stokking, R., Ikram, M.A., Vernooij, M.W., Breteler, M.M., Niessen, W.J., 2007. Multi-spectral brain tissue segmentation using automatically trained k-Nearest-Neighbor classification. Neuroimage 37, 71–81.